MRS Communications

DOI: 10.1557/s43579-022-00240-2

A useful approach to understand the origin of defects in transparent YAG ceramics

Francesco Picelli[1,2], Valentina Biasini[1], Jan Hostaša[1], Andreana Piancastelli[1], Laura Esposito[1]

[1]CNR-ISTEC, Institute of Science and Technology for Ceramics, via Granarolo 64, Faenza (RA), Italy

[2]Università degli studi di Parma, Via Università 12, Parma (PR), Italy

Corresponding author: Laura Esposito laura.esposito@istec.cnr.it

Abstract

Polycrystalline yttrium aluminum garnet (YAG, $Y_3Al_5O_{12}$) is an alternative material to single crystals in many optical applications, among others in solid state lasers, where it can be doped with an active element and used as the gain laser medium. However, compared to the single crystal production process, the manufacturing of fully dense and defect-free polycrystalline components is still a challenge. Sintering is one of the most critical steps. To obtain transparency, sintering is performed under vacuum, since the low gas pressure favors the pore closure. The pore closure process, however, may conceal the origin of defects often coming from the starting powders, and thus the optimization of the process may be difficult.
This article describes a useful approach to understand the origin of defects in transparent YAG ceramics. An air reactive sintering process is performed at a moderate temperature (1650°C) and for a short time (4h) on four mixtures. The resulting microstructures have shown to be helpful for the understanding of the origin of the residual defects observed when the same mixtures are sintered under conventional conditions (i.e. under vacuum at high temperature).
The obtained results showed that the presence of aggregates in the starting powders is responsible of the residual porosity observed in the vacuum sintered specimens. This result could not be gathered by the microstructure observation of the vacuum sintered samples alone. In the latter only residual porosity was observed. Conversely, in the air sintered samples it was possible to relate the porosity to the presence of aggregates of starting oxide particles, which eventually under vacuum react to form YAG, but leave behind residual pores.

Keywords: YAG, $Y_3Al_5O_{12}$, transparent ceramics, microstructure, sintering

1. Introduction

Reactive sintering under vacuum is one of the most conventional processes to obtain YAG-based (yttrium aluminum garnet, $Y_3Al_5O_{12}$) transparent ceramics [1] along with the vacuum sintering of precipitated powders [2].

Prior to sintering, the powders are mixed according to the desired stoichiometry, shaped and eventually calcined to eliminate possible organic residues and water. A vacuum atmosphere is needed to favor the YAG phase formation and the complete pore closure by lowering the gas pressure in the pores and

providing an additional driving force for diffusion. A molybdenum or tungsten chamber is generally used to prevent contamination especially from carbon. During the sintering cycle under vacuum, the powders react, forming intermediate phases $Y_4Al_2O_9$ (yttrium aluminum monoclinic, YAM) and $YAlO_3$ (yttrium aluminum perovskite, YAP) and finally YAG. As sintering occurs, the porosity closes [3,4].

However, a limited number of defects (mostly porosity) may still be present in the sintered ceramics, causing scattering and degrading the optical quality of the material. Vacuum sintering, despite being necessary to obtain pore-free transparent ceramics [5], often prevents the understanding of the origin of the defects in the final material. In particular, analyzing specimens sintered under these conditions, the possible presence of aggregates within the starting powders is hard to detect. During vacuum sintering the pore closure is enhanced by the decreased gas pressure within the pores, and at the same time the reaction of the single oxide powders is favored by the faster ion diffusion. Within the aggregates the reaction between Al_2O_3 and Y_2O_3 to form YAM, YAP and eventually YAG may need a longer time to complete, since the ions must diffuse for a longer distance, but eventually it completes, leading to a fully YAG-based material. In some cases however, depending on the size and degree of aggregation, residual pores can be detected because in the proximity of the aggregates the powder packing is not homogeneous, and pores with larger dimension may form which hardly close even under vacuum. On the other hand, residual porosity may also be a consequence of partial sintering, or of issues related to the shaping process.

In this sense the microstructural analysis by SEM after vacuum sintering is not helpful. It reflects the results of phenomena occurring during sintering, and gives indications on the phases present, on the grain size and on the size and amount of residual porosity [6, 7, 8, 9]. However, when the sintering is performed under high vacuum, the SEM analysis does not enable to understand the origin of the defects, e.g. what caused the residual porosity. On the other hand, the understanding of the origin of the residual porosity is fundamental for the production of defect-free transparent YAG.

Ceramics, in order to be transparent, need to exhibit a very controlled microstructure with grains of similar size and with no residual porosity [10, 11, 12]. While a number of studies analyzed the sintering conditions and the use of sintering aids in order to reach full densification of YAG ceramics [3, 13, 14, 15], more seldom the origin of the residual macro-porosity has been investigated with the intention to understand whether it forms as a consequence of the powder characteristics (size, shape, particle size distribution, presence of aggregates), of the powder processing, of the shaping steps, or the sintering conditions [4, 10, 16, 17, 18]. It is therefore of utmost importance to find a way that enables to understand the origin of these defects.

This manuscript describes an easy approach based on a simple and fast air sintering cycle, that allows to investigate the influence of the starting powder properties and the mixture processing on the final microstructure. This approach can provide all the information needed to adjust and optimize both the powder process and vacuum sintering cycle for obtaining transparent YAG based materials with superior properties. The microstructures observed after sintering at low temperature refer to the early stage of the sintering process, i.e. when the densification is not completed. In the specific case of reactive sintering, this means that the reaction among the starting oxides, is not entirely terminated. Moreover, due to the absence of vacuum, macroscopic pores do not close. In this way, it is possible to make connection between the presence of regions formed by unreacted or partially reacted powders with the residual pores, understand they origin and adjust the process accordingly (i.e. by changing the starting powders, favoring the powder mixing, changing the shaping process, etc.).

The efficacy of this approach is demonstrated by comparing the microstructures obtained with a set of powder mixtures corresponding to the stoichiometry of 10 at.% Yb:YAG. The mixtures have been prepared keeping the Y_2O_3 and Yb_2O_3 powders fixed, and changing the Al_2O_3 powders, which have a different particle

size and particle size distribution. Yb:YAG was selected as a case study, following our previous research on this material for laser gain media [8, 13].

2. Experimental

2.1. Materials preparation

The powders used are described in **Table 1**. All the powders have purity ≥99.99% except for Yb_2O_3 that has purity ≥99.9%. Four Al_2O_3 powders with different characteristics were tested.

Table 1. Properties of the oxide powders. The mean particle size values (D50) are given by the producers. The specific surface area (BET) values given by the producers are comparable to those measured in-house.

Powder	D50 [μm]	BET [m^2/g]	Particle size distribution
Al_2O_3 Sumitomo AA-1.5	1.70	1.10 [1.83 measured]	monodimensional
Al_2O_3 Baikalox CMA S050	0.77	3.1 [4.35 measured]	monodimensional
Al_2O_3 Taimei TM-DAR	0.15	14.1 [17.2 measured]	wide
Al_2O_3 Baikalox BMA15	0.12	14.7 [14.88 measured]	wide
Y_2O_3 Nippon Yttrium Compound YT4CP	1.07	20.4	wide
Yb_2O_3 Nippon Yttrium Compound YB3CP	0.523	8.6	wide

The powders were mixed in the ratio leading to the formation of 10 at.% Yb:YAG, i.e. $Yb_{0.3}Y_{2.7}Al_5O_{12}$, and the prepared mixtures are listed in

Table 2. Tetraethyl orthosilicate, TEOS, is used (0.5 wt.%) as sintering aid. The mixing was performed by ball milling with alumina milling media in absolute ethanol, followed by drying with rotavapor and sieving as already described in [19]. Pellets with a diameter of 16 mm and a thickness of 3 mm have been obtained by linear pressing at 80 MPa. The pellets have been calcinated at 800°C for 1 hour to eliminate possible humidity and organic impurities deriving from the powder processing and then cold isostatically pressed at 250 MPa.

Two sets of pellets have been prepared, one sintered in air at 1650°C with soaking time of 4 h and the other under high vacuum (10^{-4} Pa) in a furnace with W-Mo heating elements at 1750°C with a soaking time of 16 h. The sintered samples were mirror polished on both sides with diamond suspensions with grain from 15 μm to 0.25 μm.

Table 2. List of the prepared mixtures and the respective Al_2O_3 powders. All mixtures were prepared according to the stoichiometry 10 at.% Yb:YAG. The Y_2O_3 and Yb_2O_3 powders were those reported in Table 1.

Mixture	Al_2O_3 powder
1	Sumitomo AA-1.5
2	Baikalox CMA S050
3	Taimei TM-DAR
4	Baikalox BMA15

2.2 Characterization

The specific surface area of the oxide powders was measured by BET (Surfer 11510300, Thermo Scientific). The morphology of the powders and microstructure of the sintered ceramics were characterized by SEM (FE-SEM, Carl Zeiss Sigma NTS GmbH, Oberkochen, Germany) coupled with an energy-dispersive X-ray spectroscope (EDS, INCA Energy 300, Oxford Instruments, UK). The density of the pressed samples was calculated from the volume and mass, while that of sintered samples was measured by the Archimede's method in distilled water.

The optical transmittance of polished samples sintered under vacuum was measured using a UV-Vis-NIR spectrophotometer (Lambda 750, PerkinElmer Inc, US).

3. Results and discussion

Two of the Al_2O_3 powders (Sumitomo AA-1.5 and Baikalox CMA S050) were selected for their very narrow particle size distribution (**Table 1** and **Figure 1a,b**). The other two (Taimei TM-DAR and Baikalox BMA15) on the contrary, have a wide particle size distribution and are finer (**Table 1** and **Figure 1c,d**). The Y_2O_3 and Yb_2O_3 powders are both nanometric and slightly aggregated (**Figure 2**). This is reflected in the D_{50} values reported in **Table 1**, that are influenced by the agglomeration of the powders.

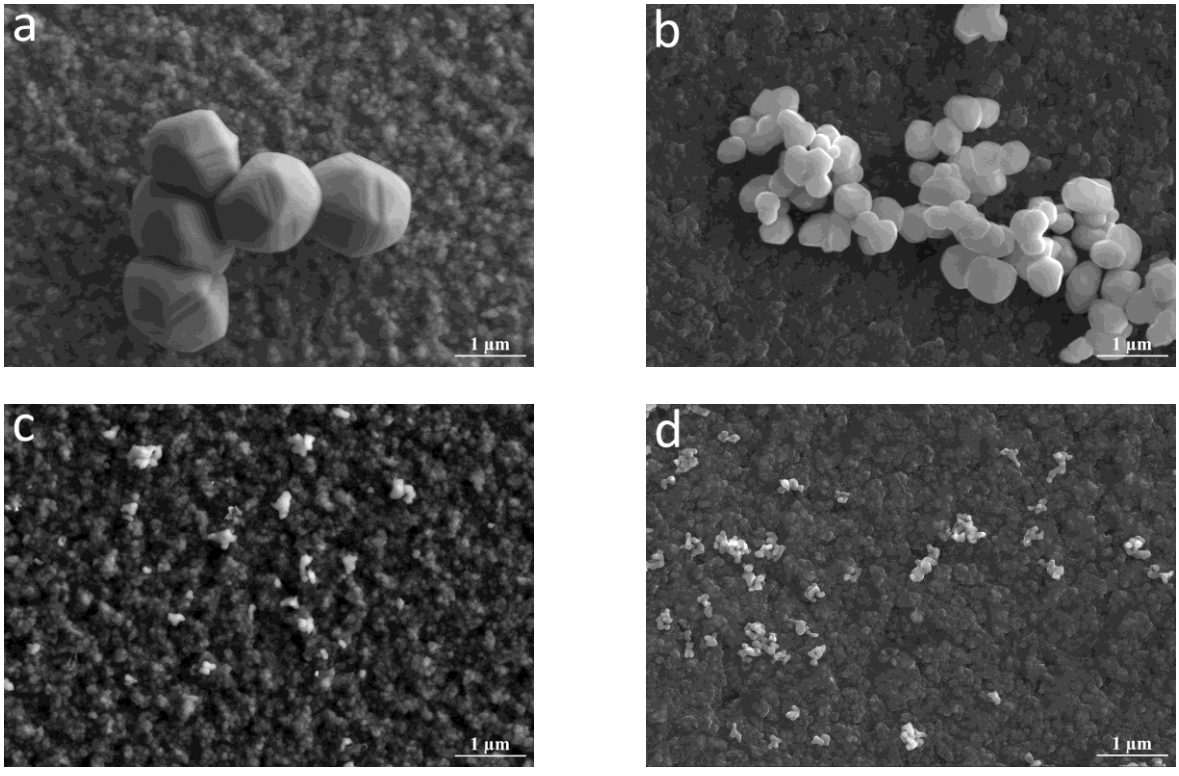

Figure 1. SEM images of the Al_2O_3 powders after sonication, (**a**) Sumitomo AA-1.5, (**b**) Baikalox CMA S050, (**c**) Taimei TM-DAR, (**d**) Baikalox BMA15.

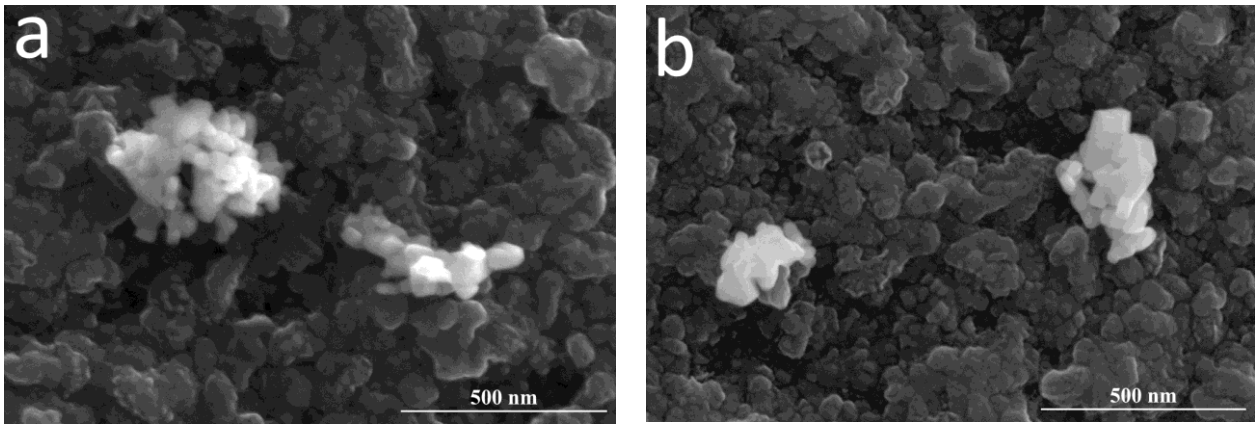

Figure 2. SEM images of the Y_2O_3 (**a**) and Yb_2O_3 (**b**) powders after sonication.

The results obtained with the mixtures listed in

Table 2

Table 2 after air sintering and vacuum sintering are summarized in **Table 3**. The microstructures obtained after air sintering are revealed in **Figure 3**, and those obtained after vacuum sintering in **Figure 4**. The optical images of the samples sintered under vacuum are reported in **Figure 5**. The optical transmittance spectrum of the samples sintered under vacuum are revealed in **Figure 6**.

Sample	Sintering atmosphere	Density (%)		Transmittance @ 1100 nm
		After Calcination	After sintering	
1a	air	59.96	98.10	n/a
2a	air	57.27	98.44	n/a
3a	air	51.69	98.21	n/a
4a	air	49.38	99.68	n/a
1v	vacuum	59.98	100	38
2v	vacuum	58.18	100	42
3v	vacuum	51.42	100	72
4v	vacuum	49.35	100	75

Table 3. Results obtained after air sintering at 1650°C × 4 h and vacuum sintering at 1750°C × 16 h. Densities have been calculated with reference to a theoretical value of 4.76 g/cm^3. The sample number refers to the mixture used, as reported in Table 2.

The samples obtained with the mixtures 1 and 2, prepared with the coarse, monodimensional Al_2O_3 powders, exhibit a higher density after calcination than the samples obtained with the mixtures 3 and 4 prepared with Al_2O_3 powders characterized by a finer and wider particle size distribution (**Table 3**). The coarse Al_2O_3 powders have a regular shape and size that favors a close particle packing and hence increase pressed the density. On the other hand, after air sintering, the density is approximately the same. In terms of microstructure, after air sintering the samples obtained with the mixtures 1 and 2 show macroscopic defects, formed by aggregated Y_2O_3-rich particles, dispersed Al_2O_3 particles and several pores, unevenly

distributed along the interface or within the aggregates (**Figure 3a,b**). The compositions of the aggregates revealed by the EDS analysis correspond to the intermediate phases that form prior to YAG from the reaction between Y_2O_3 and Al_2O_3 (**Figure 3b**). This is in agreement with the observations of Kupp *et al.* [4] for dopant-free YAG ceramics prepared by reactive sintering. During vacuum sintering these aggregates eventually evolve in YAG.

Samples obtained after air sintering with the mixtures 3 and 4, on the contrary, are formed almost entirely by the YAG phase and only few Al_2O_3 grains are found (**Figure 3c,d**). The latter were smaller in mixture 3 than in mixture 4. The residual porosity of these samples is homogeneously distributed and the pores have approximately the same size.

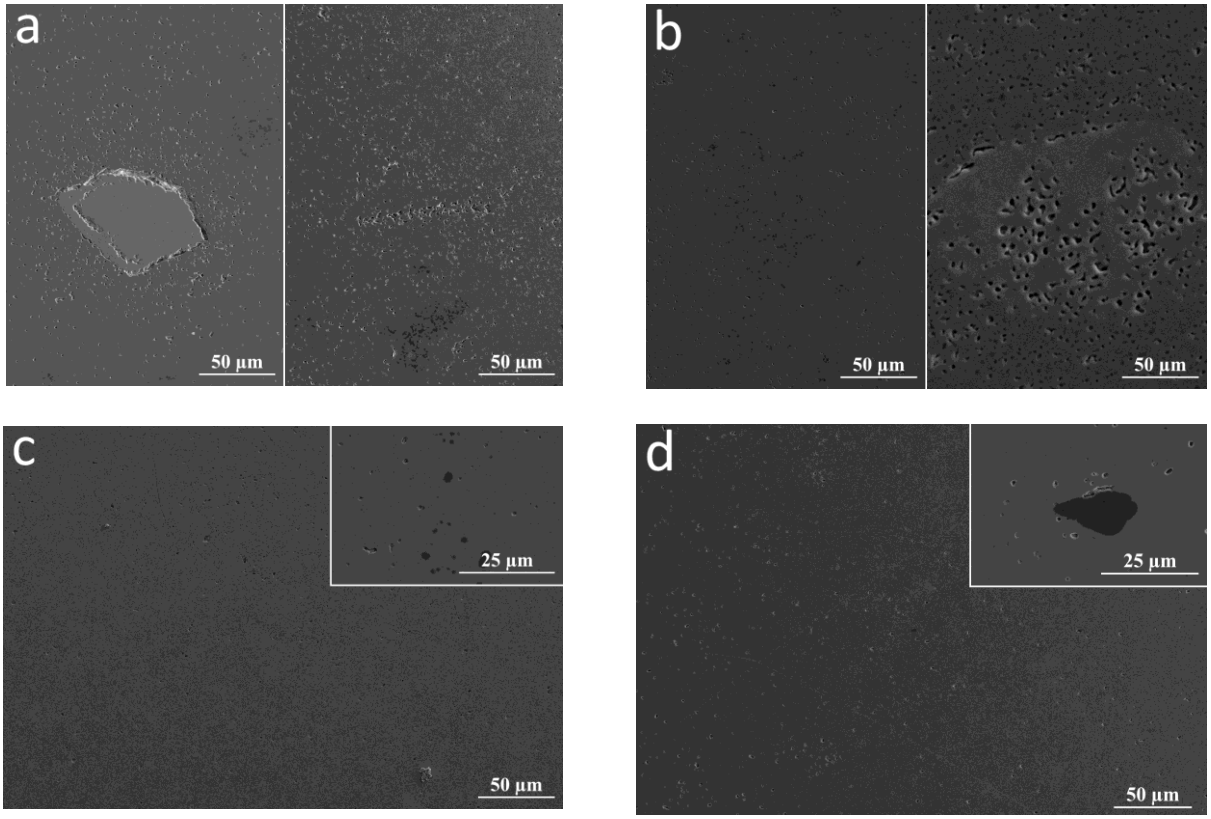

Figure 3. SEM microstructure of the polished section of the samples described in Table 3, after air sintering at 1650°C for 4 h; (**a**) 1a, (**b**) 2a, (**c**) 3a, (**d**) 4a.

The density of all samples treated under high vacuum measured with the Archimede's method reached 100 % of the theoretical value (**Table 3**, **Figure 4**, 5). This measurement, however, is not sufficiently accurate for densities approaching the theoretical one, as in the present case. Some residual porosity was observed with SEM in all the samples, and the measured in-line transmittance values confirm the presence of some scatterers, although the amount is apparently low and does not affect the density measurements (**Figure 6**). Some macroscopic defects are present in the samples obtained from mixtures 1 and 2 (**Figure 4a,b**) These defects are mainly formed by large pores, whereas in terms of compositions only YAG grains could be detected. The formation of these large pores is a consequence of the uneven distribution of porosity that forms around the Y_2O_3–rich aggregates during the sintering process, and that has been clearly observed after air sintering (**Figure 3a,b**). Under vacuum, these pores coalesce, forming few large pores. They do not disappear despite the vacuum atmosphere, because within the aggregates the reaction that leads to the

YAG formation is slowed down and once it is concluded, the residual porosity is of the closed type. Closed pores are more prone to coalesce than to disappear, especially when their size is bigger than the size of the surrounding grains, as in the present case (the pores are in the range of 50 µm and the grains of 20 µm). In addition, during the sintering process, the YAG formation within the aggregates is slowed down because the Y_2O_3 particles are not in mutual contact with the Al_2O_3 particles, as in the case of the homogeneous powder mixtures.

Samples obtained with mixtures 3 and 4 on the contrary, showed a more regular microstructure, with very few residual pores (**Figure 4c,d**).

As expected, the transmittance reflects the microstructural defects, being higher in the case of samples obtained with mixtures 3 and 4 and lower in the case of mixtures 1 and 2 (Table 3, **Figure 6**). However, while it is possible to estimate the transmittance from the microstructure (i.e. from the amount and size of pores and defects) [20], transmittance *per se* provides less information about the size distribution of the scatterers [12] and even less about their possible origin.

This investigation shows that the air sintering approach enables to understand the origin of the residual defects observed after vacuum sintering. If for example samples formed by mixtures 1 and 2 had been sintered solely under vacuum, it would have been not possible to understand that the macroscopic residual pores shown in **Figure *4*a,b** were a consequence of the Y_2O_3-rich aggregates since these fully disappear under vacuum.

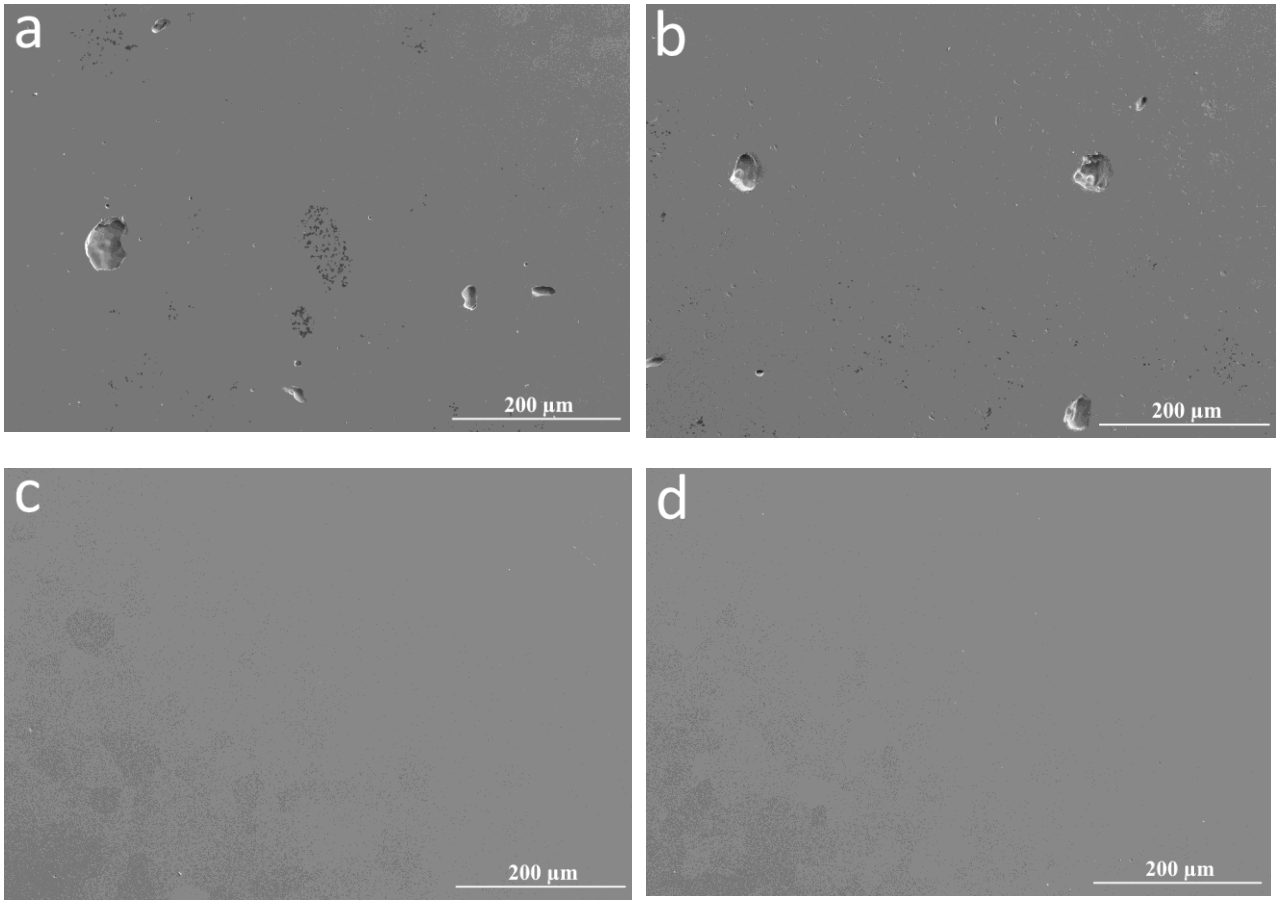

Figure 4. SEM microstructure of the polished surfaces of the samples described in Table 3, after vacuum sintering at 1750°C for 16 h; (**a**) 1v, (**b**) 2v, (**c**) 3v, (**d**) 4v.

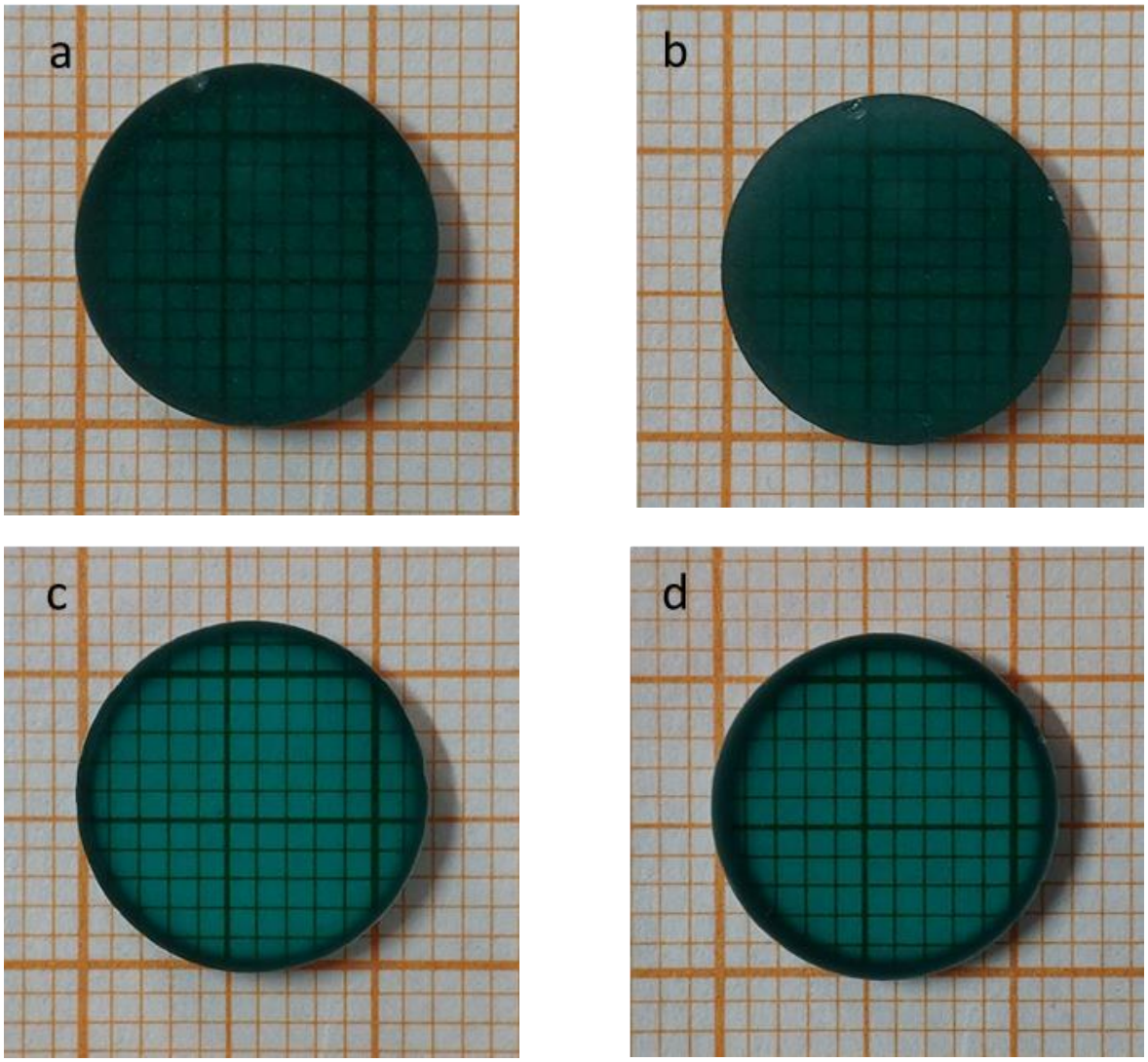

Figure 5. Optical images of the samples described in Table 3 after vacuum sintering at 1750°C for 16 h; (**a**) 1v, (**b**) 2v, (**c**) 3v, (**d**) 4v.

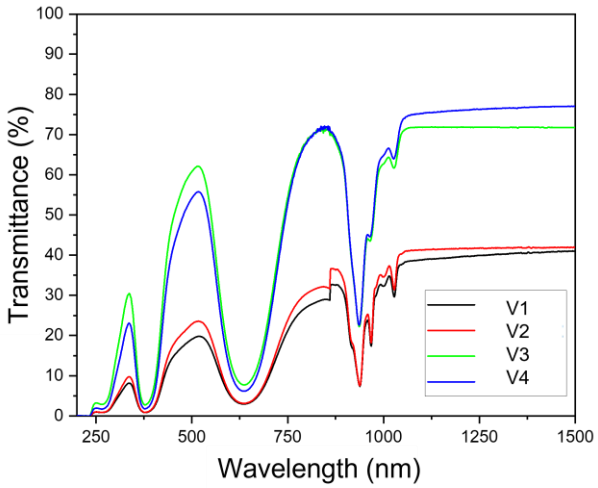

Figure 6. Optical transmittance curves measured in the wavelength range 200 – 1500 nm on polished samples sintered under vacuum (Table 3).

Moreover, from this study emerges that, when using coarser monodimensional Al_2O_3 powders in combination with nanometric Y_2O_3 and Yb_2O_3 powders, particular care must be put in the processing of the powder. In fact, despite the same Y_2O_3 powder was used in all samples and all mixtures were processed under the same mixing conditions, no Y_2O_3-rich aggregate was observed when Al_2O_3 powders characterized by a wider particle size distribution were used. Hence, monodimensional Al_2O_3 powders inhibit the extensive, intimate mixing among all powders, which in turn is achieved with Al_2O_3 powder characterized by a fine and wide particle size distribution. This is in line with the observation of Yavetskiy et al. [21] of the positive effect of a bimodal distribution of Y_2O_3 powder on the densification of reactively sintered Nd:YAG. As a result, a useful indication that is derived from this study is, for example, that the use of a dispersant when using a monodimensional Al_2O_3 powder in combination with nanometric Y_2O_3 and Yb_2O_3 powders may favor their intimate mixing.

4. Conclusions

The proposed method to investigate the microstructure of YAG ceramics partially sintered in air, reveals information that, otherwise, is lost after vacuum sintering. It was shown that the particle packing and the presence of aggregates in the green body are easier to evaluate from the microstructure of samples sintered in air. In the analysed systems this approach provided a better understanding of the origin of defects present in the vacuum-sintered materials. The combination of monodimensional coarser Al_2O_3 powders with nanometric Y_2O_3, for example, led to an increased presence of defects compared to the mixtures with a finer Al_2O_3 with a wider particle size distribution.

Acknowledgements

The authors gratefully acknowledge the support from the Italian Ministry of Defence under PNRM Contract No. 8731 of 04/12/2019 (CeMiLAP2).

Conflicts of interest statement

The Authors declare that they have no affiliation or involvement in any organization or entity with any financial interest or non-financial interest in the subject matter discussed in this manuscript.

Data availability statement

The Authors declares that datasets generated during and/or analysed during the current study are available from the corresponding author on reasonable request.

References

[1] S.-H. Lee, S. Kochawattana, G. L. Messing, J. Q. Dumm, G. Quarles, V. Castillo, Solid-state reactive sintering of transparent polycrystalline Nd:YAG ceramics, J. Am Ceram. Soc. 89 (2006) 1945–1950. DOI: 10.1111/j.1551-2916.2006.01051.x

[2] X. Chen, T. Lu, N. Wei, T. Hua, Q. Zeng, Y. Wu, Fabrication and microstructure development of Yb:YAG transparent ceramics from co‐precipitated powders without additives, J Am Ceram Soc. 102 (2019) 7154–7167. DOI: 10.1111/jace.16635

[3] R. Boulesteix, A. Maître, L. Chrétien, Y. Rabinovitch, C. Sallé, Microstructural evolution during vacuum sintering of yttrium aluminium garnet transparent ceramics: toward the origin of residual porosity affecting the transparency, J. Am. Ceram. Soc. 96 (2013) 1724–1731.DOI: 10.1111/jace.12315

[4] E. R. Kupp, S. Kochawattana, S.-H. Lee, S. Misture, G. L. Messing, Particle size effects on yttrium aluminum garnet (YAG) phase formation by solid-state reaction, J. Mater. Res. 29 (2014) 2303–2311. DOI: 10.1557/jmr.2014.224

[5] A. Ikesue, Y. L. Aung, T. Taira, T. Kamimura, K. Yoshida, G. L. Messing, Progress in ceramic lasers, Annu. Rev. Mater. Res. 36 (2006) 397–429. DOI: 10.1146/annurev.matsci.36.011205.152926

[6] R. Boulesteix, A. Maître, J.-F. Baumard, Y. Rabinovitch, Quantitative characterization of pores in transparent ceramics by coupling electron microscopy and confocal laser scanning microscopy, Mater. Lett. 64 (2010) 1854–1857. DOI: 10.1016/j.matlet.2010.05.028

[7] A.J. Stevenson, X. Lin, M.A. Martinez, J.M. Andreson, D.L. Suchy, E.R. Kupp, E.C. Dickey, K.T. Muller, G.L. Messing, Effect of SiO_2 on densification and microstructure development in Nd:YAG transparent ceramics, J. Am. Ceram. Soc 94 (2011) 1380-1387. DOI: 10.1111/j.1551-2916.2010.04260.x

[8] L. Esposito, T. Epicier, M. Serantoni, A. Piancastelli, D. Alderighi, A. Pirri, G. Toci, M. Vannini, S. Anghel, G. Boulon, Integrated analysis of non-linear loss mechanisms in Yb:YAG ceramics for laser applications, J. Eur. Ceram. Soc. 32 (2012) 2273–2281. DOI: 10.1016/j.jeurceramsoc.2012.02.047

[9] T. Uhlířová, J. Hostaša, W. Pabst, Characterization of the microstructure of YAG ceramics via stereology-based image analysis, Ceramics-Silikáty 58 (2014) 173-183.

[10] A. Ikesue, K. Yoshida, T. Yamamoto, I. Yamaga, Optical scattering centers in polycrystalline Nd:YAG laser, J. Am. Ceram. Soc. 80 (1997) 1517–1522. DOI: 10.1111/j.1151-2916.1997.tb03011.x

[11] A. Krell, J. Klimke, T. Hutzler, Transparent compact ceramics: Inherent physical issues, Opt. Mat 31 (2009) 1144-1150. DOI: 10.1016/j.optmat.2008.12.009

[12] W. Pabst, J. Hostaša, L. Esposito, Porosity and pore size dependence of the real in-line transmission of YAG and alumina ceramics, J. Eur. Ceram. Soc. 34 (2014) 2745-2756. DOI: 10.1016/j.jeurceramsoc.2013.12.053

[13] J. Hostaša, L. Esposito, D. Alderighi, A. Pirri, Preparation and characterization of Yb-doped YAG ceramics, Opt. Mater. 35 (2013) 798–803. DOI: 10.1016/j.optmat.2012.05.028

[14] J. Li, J. Liu, B. Liu, W. Liu, Y. Zeng, X. Ba, T. Xie, B. Jiang, Q. Liu, Y. Pan, X. Feng, J. Guo, Influence of heat treatment of powder mixture on the microstructure and optical transmission of Nd:YAG transparent ceramics, J. Eur. Ceram. Soc. 34 (2014) 2497-2507. DOI: 10.1016/j.jeurceramsoc.2014.03.004D

[15] J. Hostaša, F. Picelli, S. Hříbalová, V. Nečina, Sintering aids, their role and behaviour in the production of transparent ceramics, Open Ceram. 7 (2021) 100137. DOI: 10.1016/j.oceram.2021.100137

[16] J. Liu, L. Lin, J. Li, J. Liu, Y. Yuan, M. Ivanov, M. Chen, B. Liu, L. Ge, T. Xie, H. Kou, Y. Shi, Y. Pan, J. Guo, Effects of ball milling time on microstructure evolution and optical transparency of Nd:YAG ceramics, Ceram. Int. 40 (2014) 9841-9851. DOI: 10.1016/j.ceramint.2014.02.076

[17] A. Goldstein, A, Krell, Transparent Ceramics at 50: Progress Made and Further Prospects, J. Am. Ceram. Soc. 99 (2016) 3173-3197. Doi: 10.1111/jace.14553

[18] A. Ikesue, K. Yoshida, T. Yamamoto, I. Yamaga, Optical scattering centers in polycrystalline Nd:YAG laser, J. Am. Ceram. Soc. 80 (1997) 1517-1522. DOI: 10.1111/j.1151-2916.1997.tb03011.x

[19] L. Esposito, A. Piancastelli, A. L. Costa, M. Serantoni, G. Toci, M. Vannini, Experimental features affecting the transparency of YAG ceramics, Opt. Mat. 33 (2011) 713-721. DOI: 10.1016/j.optmat.2010.09.016

[20] S. Hříbalová, W. Pabst, Modeling light scattering by spherical pores for calculating the transmittance of transparent ceramics – All you need to know, J. Eur. Ceram. Soc. 41 (2021) 2169-2192. DOI: 10.1016/j.jeurceramsoc.2020.11.046

[21] R.P. Yavetskiy, V.N. Baumer, A.G. Doroshenko, Yu L. Kopylov, D. Yu. Kosyanov, V. B. Kravchenko, S.V. Parkhomenko, A.V. Tolmachev, Phase formation and densification peculiarities of $Y_3Al_5O_{12}$:Nd^{3+} during reactive sintering, J. Cryst. Growth 401 (2014) 839–843. DOI: 10.1016/j.jcrysgro.2014.01.034